ACS APPLIED MATERIALS & INTERFACES

Research Article

www.acsami.org

Highly Stable and Sensitive Paper-Based Bending Sensor Using Silver Nanowires/Layered Double Hydroxides Hybrids

Yong Wei, Shilong Chen, Fucheng Li, Yong Lin, Ying Zhang, and Lan Liu*

College of Materials Science and Engineering, Key Lab of Guangdong Province for High Property and Functional Macromolecular Materials, South China University of Technology, Guangzhou 510641, P. R. China

Supporting Information

ABSTRACT: Highly sensitive flexible piezoresistive materials using silver nanowires (AgNWs) composites have been widely researched due to their excellent electrical, optical, and mechanical properties. Intrinsically, AgNWs tend to aggregate in polymer matrix because of the intense depletion-induced interactions, which seriously influence the percolation threshold of the composites. In this study, we report a highly stable and sensitive paper-based bending sensor using the AgNWs and layered double hydroxides (LDHs) to construct a hybrid conductive network in waterborne polyurethane that is easy to destruct and reconstruct under bending deformation. The nonconductive 2D LDH nanosheets are embedded into AgNWs network and assist dispersion of AgNWs, which depends on the hydrogen bonding between the two nanostructures. The percolation threshold of the composites decreases from 10.8 vol % (55 wt %) to 3.1 vol % (23.8 wt %), and the composites reaches a very low resistivity (10^{-4} Ω·cm) with a small amount of AgNWs (8.3 vol %) due to the dispersion improvement of AgNWs with the effect of LDH nanosheets. The as-prepared conductive composites with low percolation threshold can be manufactured on paper via various methods such as rollerball pen writing, inkjet printing, or screen printing. The bending sensor prepared by manufacturing the composites on paper shows low-cost, excellent conductivity, flexibility (>3000 bending cycles), sensitivity (0.16 rad^{-1}), fast response (120 ms) and relaxation time (105 ms), and nontoxicity. Therefore, a simple but efficient wearable sensor is developed to monitor the human motions (such as fingers and elbow joints movements) and presents good repeatability, stability, and responsiveness, making the bending sensor possibly able to meet the needs in numerous applications for robotic systems.

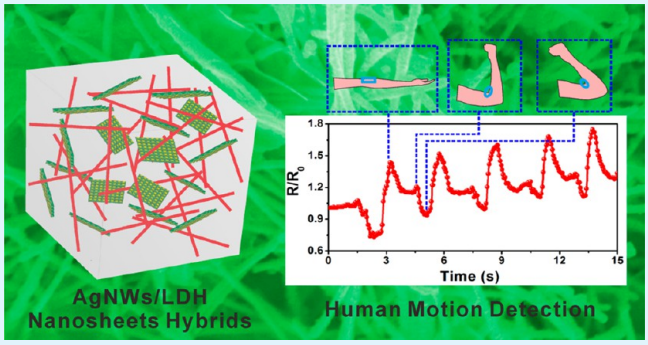

KEYWORDS: *bending sensor, human motion detection, silver nanowires composites, layered double hydroxides, hybrids*

INTRODUCTION

Flexible piezoresistive materials (FPR materials) have attracted considerable attention due to their extensive applications in wearable electronics, robotic systems, electronic skin, et al.[1−8] FPR materials can be easily obtained by manufacturing flexible conductive composites (FCCs) on various natural or synthetic flexible substrates. Paper is a widely used flexible substrate that is biodegradable and recyclable because it is made up of environmentally friendly raw materials.[9] The flexibility of paper is superior to the common plastic substrates such as poly(ethylene terephthalate) (PET) or polyimide (PI) as it is not only bendable and rollable but can be folded and unfolded as well.[10] Moreover, FCC can be manufactured on paper substrate by writing, screen printing, or inkjet printing. Also, paper is lightweight, and the price of paper is lower than that of plastic substrates.[11] Therefore, paper has been considered as a new ideal substrate to make flexible electronics.

FCC is usually prepared by incorporating conductive fillers into the flexible polymer matrix such as poly(vinylidene fluoride) (PVDF),[12] poly(dimethylsiloxane) (PDMS),[13,14] waterborne polyurethane (WPU),[15] and nitrile butadiene rubber (NBR).[16] The electrical connection of conductive fillers in polymer matrix is determined by the percolation theory and conductive current passes constructed by the junctions of conductive fillers.[17] The percolation theory points out that a typical piezoresistive behavior can be generally observed at the filler concentration beyond the percolation threshold, in which the formed initial conductive network reconstructs under external stimuli such as bending, stretching, and compression. To maintain the high sensitivity and conductivity of FPR materials, many studies have focused on decreasing the percolation threshold of FCC.[18,19] It is generally accepted that the morphology and size of conductive fillers play an important role in determining the percolation threshold. For instance, conductive composites incorporated with one-dimensional (1D) conductive fillers (nanowires or nanotubes) often exhibit lower percolation threshold.[20] Silver nanowires (AgNWs) possess the highest electrical and thermal conductivity among metal nanowires and are highly resistant to

Received: January 7, 2015
Accepted: June 17, 2015
Published: June 17, 2015

DOI: 10.1021/acsami.5b03824
ACS Appl. Mater. Interfaces 2015, 7, 14182−14191

oxidation and corrosion. Moreover, AgNWs with high aspect ratio still retain outstanding conductivity while bending, rolling, or twisting. Although AgNWs applied in conductive composites form conductive network more easily than silver flakes or nanoparticles, the percolation threshold is strongly dependent on the distribution of AgNWs in polymer matrix. Unfortunately, AgNWs tend to aggregate in polymer matrix due to the strong depletion-induced interaction; thus, more AgNWs are needed to obtain conductive composites with high conductivity that leads to higher percolation threshold. Therefore, improving the dispersion of AgNWs in polymer matrix is the key to decreasing the percolation threshold. It is reported that nonconductive zero-dimensional silica nanoparticles are introduced and the concentration of AgNWs is down to 2 vol % and still obtains the resistivity of 10^{-4} Ω·cm.[21] In addition, hybrids of two-dimensional (2D) graphene and AgNWs are also performed and serve as conductive filler to epoxy resin, the percolation threshold decreasing from 30 to 10 wt % due to the synergistic effect of graphene and AgNWs.[22]

In this Article, hybrids of nonconductive 2D Co−Al layered double hydroxides (LDHs) nanosheets and 1D AgNWs were prepared and incorporated into WPU. The LDH nanosheets assisted dispersion of AgNWs in WPU was described. Using AgNWs/LDH nanosheets hybrids as conductive filler, it can decrease the percolation threshold from 10.8 vol % (55 wt %) to 3.1 vol % (23.8 wt %), and the resistivity reaches $(2.5 \pm 0.3) \times 10^{-4}$ Ω·cm only incorporated with 8.3 vol % AgNWs. The rollerball pen loaded with the as-prepared conductive ink could write on paper, and the conductive text or tracks could be obtained to be applied in flexible electric circuits. The bending sensor fabricated by manufacturing the conductive ink on paper shows excellent flexibility (over 3000 bending cycles) and high sensitivity (0.16 rad^{-1}) to bending deformation and can be used as wearable bending sensors. Such sensors can be mounted onto human bodies to monitor the motion of fingers and joints. Moreover, the simple but efficient fabrication process in this study makes it possible for large-scale and large-area preparation of the flexible bending sensors.

EXPERIMENTAL SECTION

Materials. Silver nitrate ($AgNO_3$) was bought from Tianjin Qilun Chemical Technology Co., Ltd. Poly(vinylpyrrolidone) (PVP, M_w = 1 300 000 g/mol) was bought from J&K Technology Co., Ltd. (Beijing, China). Glycerol, ethylene glycol, formamide, hydrogen chloride (HCl), sodium nitrate ($NaNO_3$), and anhydrous ethanol were purchased from Tianjin Fuyu Fine Chemical Co., Ltd. (Tianjin, China). Sodium chloride (NaCl), cobalt chloride ($CoCl_2·6H_2O$), and aluminum chloride ($AlCl_3$) were purchased from Tianjin Fuchen Chemical Reagents Factory (Tianjin, China). Waterborne polyurethane (WPU, solid content is 30 wt %) was supported by Guangzhou Bihong Chemical Technology Co., Ltd.

Synthesis of AgNWs. The AgNWs used in this research were synthesized by a mediated glycerol process.[23] Typically, 2.9 g of PVP was added to 100 mL of glycerol in a 250 mL three-necked flask with gentle stirring for 12 h at 100 °C until all PVP was dissolved. After the temperature cooled down to room temperature, 4.65 mL ethylene glycol solutions of $AgNO_3$ (1.0 M) were added to the flask, and then 30 mg of NaCl dissolved in 0.3 mL of H_2O was dropped in. After that, the flask was immersed in an oil bath, and the temperature was raised to 180 °C and kept for 2.0 h. The uniform gray−green color of solutions indicates successful synthesis of AgNWs. The AgNWs were separated by centrifugation process using anhydrous ethanol three times, and the final product was dispersed in anhydrous ethanol with a concentration of 5.0 mg·L^{-1}.

Liquid Exfoliation of Co−Al LDHs. The hexagonal Co−Al LDHs were synthesized by the typical hydrothermal process.[24] To exfoliate the Co−Al LDHs, the pristine Co−Al LDHs were anion exchanged with a salt−acid treatment.[25] After that, 0.1 g of anion-exchanged LDHs sample was dispersed into 100 mL of formamide and vigorously stirred at ambient temperature for 48 h under nitrogen gas, and the unexfoliated LDHs particles were removed by centrifugation at 2000 rpm for 10 min. Finally, the pink, transparent colloidal suspension of Co−Al LDH nanosheets was obtained and diluted to 0.5 mg/mL.

Hybridization of AgNWs and LDH Nanosheets and Preparation of Writable and Printable Conductive Ink. Hybrids of AgNWs and LDH nanosheets were prepared via dropping LDH nanosheets suspensions into AgNWs suspensions in a 100 mL beaker and careful shaking. The precipitates were collected by centrifugation, and gel-like AgNWs/LDH nanosheets hybrids were obtained. The collected gel-like AgNWs/LDH nanosheets hybrids were directly mixed with WPU and homogenized, and then writable and printable conductive ink was acquired after the viscosity was adjusted. To prepare the conductive ink filled with AgNWs only, AgNWs suspension was mixed with WPU and homogenized, and the mixture was concentrated by rotary evaporation at 60 °C for 2 h (this may cause some loss of AgNWs).

Preparation of Paper-Based Wearable Bending Sensor. To prepare the bending sensor, the conductive ink incorporated with the hybrids (the mass ratio of WPU, AgNWs, and LDH nanosheets was 4:4:1 to reach a low resistivity) was manufactured on paper by screen printing and dried in an oven at 60 °C for 12 h. The thickness, width, and length of the sensor were 50 μm, 3 mm, and 6 cm, respectively. At the same time, the copper electrodes were fixed at the two terminals by silver paste (YH 2008, HongKong Yihui Co., Ltd.). The sensor based on composites incorporated with AgNWs only (18.8 vol % AgNWs was mixed with WPU to make the resistivity reach 10^{-4} Ω·cm) was also prepared as a contrast.

Characterization. The UV−vis absorption spectroscopy was taken at room temperature on a HP 8453E spectrometer (HP Co. Ltd., U.S.). X−ray diffraction (XRD) analysis was conducted using a Bruker D8 ADVANCE diffractometer (Bruker Co. Ltd., Billerica, MA) with Ni-filtered Cu−Kα radiation (λ = 0.154 18 nm) with a scanning speed of 2°/min at 40 kV and 40 mA. The transmission electron microscopy (TEM) images were taken by JEOL JEM-2100HR instrument (EDAX Inc., Mahwah, NJ) operated at 100 kV. The morphology of AgNWs, LDHs, and composites were observed through a Nano SEM 430 instrument (FEI Co. Ltd., Hillsboro, OR). The weight loss result was measured by TA Instruments (TA Co. Ltd., Pennsylvania, PA). X-ray photoelectron spectroscopy (XPS) analysis was carried out using a Kratos Axis Ultra DLD electron spectrometer (Kratos Co. Ltd., Manchester, England). Fourier transform infrared spectroscopy (FTIR) spectrum was collected by a Bruker VERTEX70 FTIR spectrometer (Bruker Co. Ltd., Billerica, MA) at room temperature using KBr disc technique. The resistance (ρ, Ω) of the composite was measured by a TEGAM 1740 microohmmeter, and the bulk resistivity (R, Ω·cm) of composite was calculated via the following equation: $R = \rho S/L$, where L (cm) and S (cm^2) are the length and cross-sectional area of the sample, respectively. Conversion between the mass fraction and volume fraction of the fillers can be performed by the following equation[22,26]

$$v = \frac{w\rho_{LDH}\rho_{WPU}}{w\rho_{WPU}(\rho_{LDH} + \gamma\rho_{Ag}) + [1 - w(1 + \gamma)]\rho_{Ag}\rho_{LDH}}$$

where v and w are the volume fraction and mass fraction of the filler, respectively; ρ_{Ag}, ρ_{LDH}, and ρ_{WPU} are the density of AgNWs (10.5 g·cm^{-3}), LDH nanosheets (2.7 g·cm^{-3}), and WPU (1.05 g·cm^{-3}), respectively; and γ is the mass ratio of LDH nanosheets and AgNWs. The bending performance was measured by bending the sensor with a radius of 0.5 cm under the frequency of 4 Hz, and the resistance was real-time monitored by TEGAM 1740 microohmmeter. To measure the sensitivity (S) of the sensor, the resistance response of the sensor to bending angle (θ) from 0° to 180° was recorded, and the sensitivity was calculated via the following equation: $S = (\Delta R/R_0)/\theta$,[4] where ΔR is the initial resistance (R_0) minus the measured resistance (R). It is difficult to obtain the accurate value of the response and relaxation time. In this

DOI: 10.1021/acsami.5b03824
ACS Appl. Mater. Interfaces 2015, 7, 14182−14191

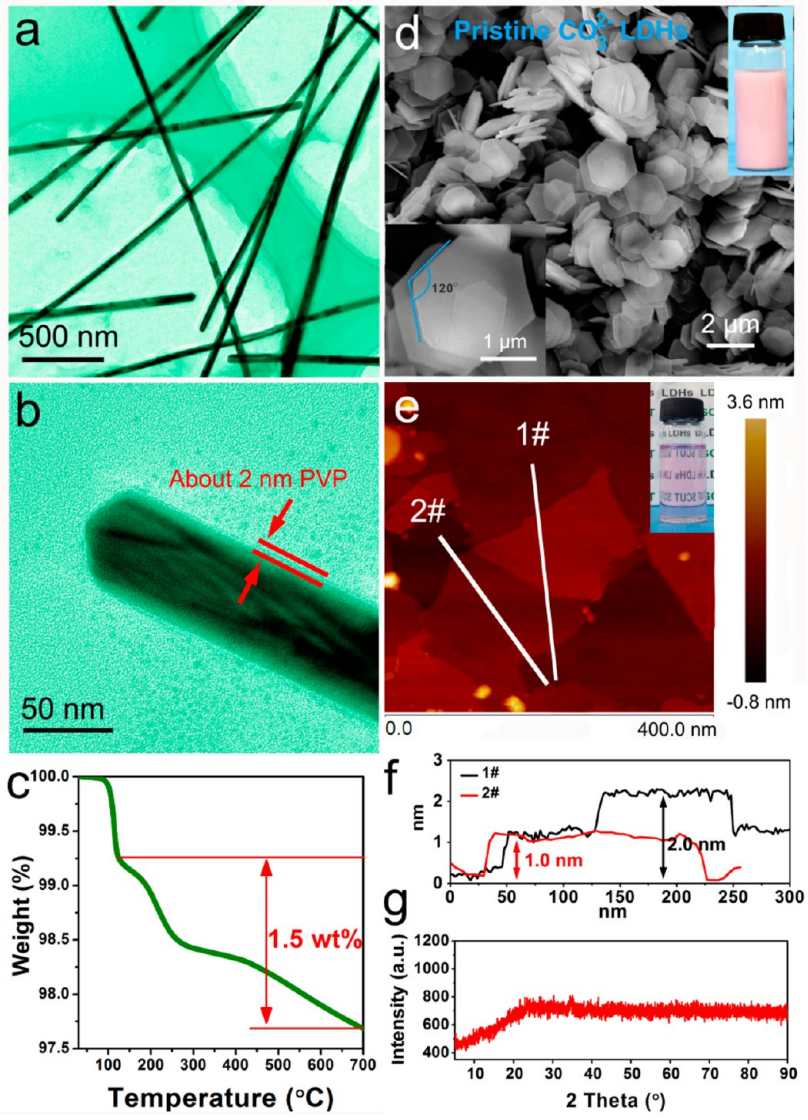

Figure 1. (a and b) TEM images of as-prepared AgNWs with different magnifications to show the morphology and surface of AgNWs. (c) TG results of pristine AgNWs. (d) FESEM image of pristine Co−Al LDHs; the inset is the SEM image of Co−Al LDHs with higher magnification and digital photograph of pristine LDH aqueous suspension. (e) Tapping-mode AFM image of LDH nanosheets deposited on a fresh mica substrate; the inset is the digital photograph of the LDH nanosheets colloidal suspension. (f) Height profile along the two lines in (e). (g) XRD pattern for the exfoliated Co−Al LDH nanosheets obtained after centrifugation from LDH colloidal suspension.

research, the approximate response and relaxation time of the sensor was measured by bending the sensor to 90° as soon as possible (<30 ms), and the real-time resistance was collected and the response and relaxation time was defined as the time interval between 10% and 90% of the steady state values.[27] To monitor the motion of fingers and joints, the sensor 3 mm in width and 6 cm in length was mounted on fingers or joints by strong glue (Pattex PXT4X). While testing, the two terminals of the sensor were fixed on fingers or joints by 3M Scotch tape to avoid the resistance instability of the contact between the electrode and the sensor.

RESULTS AND DISCUSSION

Preparation of AgNWs and Co−Al LDH Nanosheets. Uniform AgNWs with 20 ± 5 μm length and 50 ± 5 nm diameter were synthesized (Supporting Information Figure S1). The XRD pattern (Supporting Information Figure S2) confirmed that the AgNWs are highly crystalline and exhibit purely in a face-centered cubic (fcc) phase. TEM image with higher magnification (Figure 1a and b) shows that about 2 nm thick PVP existed on the surface of pristine AgNWs. The TG result shows that the continuous weight loss of as-prepared AgNWs starting at about 100 °C is assigned to the decomposition of PVP, and it is unfinished even up to 700 °C (Figure 1c). Figure 1d shows typical FESEM images of pristine Co−Al LDHs. As can be seen, the LDHs with hexagonal shape have a lateral size about 2 μm. The LDH nanosheets were liquid exfoliated in formamide.[25] The XRD pattern of LDH nanosheets is shown in Figure 1g; the sharp basal diffraction peaks of pristine LDH are almost absent, indicating the collapse of the ordered layered structure of the pristine Co−Al LDHs. The two-dimensional tapping-mode AFM image (Figure 1e) shows that the particle size is about 200−400 nm. The height profiles (Figure 1f) reveal that the nanosheets have an average thickness of about 1.0 nm, demonstrating that single layer LDH nanosheets were obtained.

Hybridization of AgNWs and LDH Nanosheets. Figure 2a shows the schematic of preparation of AgNWs/LDH nanosheets hybrids. In brief, LDH nanosheets were dropwise

DOI: 10.1021/acsami.5b03824
ACS Appl. Mater. Interfaces 2015, 7, 14182−14191

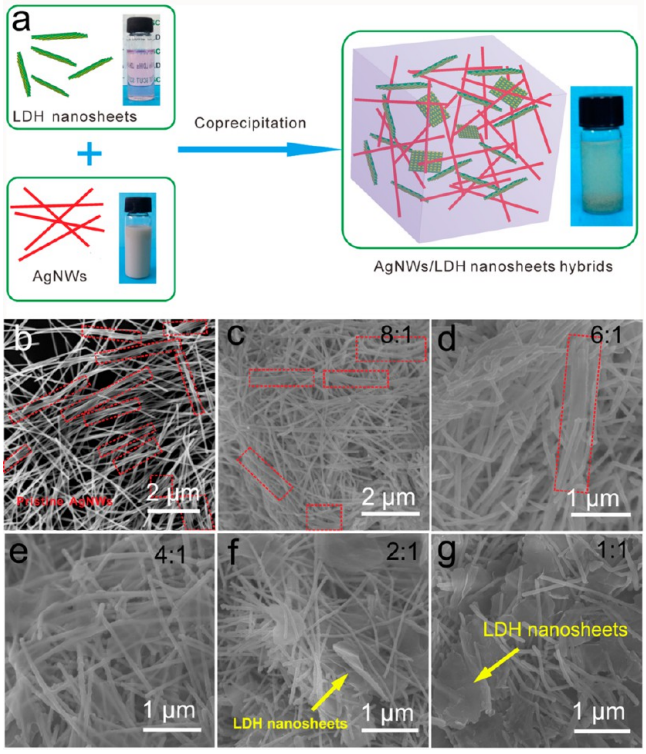

Figure 2. (a) Schematic illustration to show the preparation of AgNWs/LDH nanosheets hybrids. (b) FESEM image of as pristine AgNWs deposited on glass slides and dried in air. (c–g) FESEM images of AgNWs/LDH nanosheets hybrids with different proportion of AgNWs to LDH nanosheets from 8:1 to 1:1 (selected area in b–d shows the bundles of AgNWs).

added into AgNWs dispersion with careful shaking, and the homogeneous state of AgNWs was broken, indicating the assembling of AgNWs and LDH nanosheets. The FESEM images of AgNWs/LDH nanosheets hybrids with different proportion are shown in Figure 2b–g. As can be seen, bundles of AgNWs (more than 3 AgNWs in parallel adhered together) are clearly observed for pristine AgNWs (Figure 2b) and AgNWs/LDH nanosheets hybrids when the proportion of AgNWs and LDH nanosheets ranges from 8:1 to 6:1 (Figure 2c and d) due to the strong depletion-induced interaction existing among AgNWs. However, the AgNWs 3D network is observed, and AgNWs do not obviously aggregate when the proportion of AgNWs and LDH nanosheets ranges from 4:1 to 2:1. The LDH nanoshests are embedded into AgNWs network leading to AgNWs divided by single layer LDH nanosheets, and a hybrid 3D network is constructed (Figure 2e and f). If the concentration of LDH nanosheets is nearly equal to the AgNWs, there are excess LDH nanosheets covered on the surface of AgNWs (Figure 2g), demonstrating that excessive LDH nanosheets decrease the contact of AgNWs, which is not conducive to the formation of conductive network in polymer matrix. The analysis above indicates that LDH nanosheets can prevent AgNWs from aggregating to bundles and the optimum proportions of AgNWs and LDH nanosheets to form 3D hybrid network range from 4:1 to 2:1.

In order to further investigate the chemical nature of elements, XPS investigations for AgNWs, LDH nanosheets, and their hybrids were performed, and high-resolution spectra of C 1s, Co 2p, and Al 2p were obtained from the survey of wide-scan spectra (Figure 3). As illustrated in Figure 3, all the spectra are referenced to C 1s peak (binding energy = 284.6 eV).[28] Beside the main peak at 284.6 eV for C−C and 285.3 eV for C−N, a broader peak and a higher binding energy corresponding to the C═O are observed after hybridization due to the charge transfer from AgNWs to the surface of LDH nanosheets. The XPS of the Co 2p region can be fitted into four peaks, the first two peaks at 781.4 and 784.9 eV ascribed to Co 2p3/2 and its shakeup satellite and the other two peaks at 795.4 and 801.2 eV assigned to the Co 2p1/2 and its shakeup satellite.[29] After hybridization, these four peaks shift to 779.3, 786.0, 797.5, and 803.4 eV, respectively. In addition, the XPS of Al 2p shifts from 72.3 to 74.2 eV. The UV−vis spectrum Supporting Information Figure S7) of pristine AgNWs shows two clear SPR peaks at 350.7 and 377.1 nm corresponding to the longitudinal and transverse mode of AgNWs, respectively.[30] As is seen, these two peaks shift to 354.5 nm and 382.7 nm after hybridization. Since a thin layer PVP molecule (about 2 nm) is absorbed on the surface of AgNWs during the crystal growing process[31,32] and a large number of hydroxyl groups on the host layer of LDH nanosheets (the formula of LDHs can be described as $[M^{II}_{1-x}M^{III}_{x}(OH)_2]^{x+}(A^{n-})_{x/n}\cdot mH_2O$),[33] hydrogen bonding can be formed between the carbonyl group (C═O) of PVP on the surface of AgNWs and hydroxyl groups (−OH) on the host layers of LDH nanosheets.

Properties of the Composites Filled with AgNWs/LDH Nanosheets Hybrids. One-dimensional conductive fillers (such as nanowires and nanotubes) often form conductive networks more easily due to the high aspect ratio. However, more than 10 vol % of 1D conductive fillers is necessary, and volume resistivity of these composites only reaches 10^{-2} Ω·cm.[21] In this research, a facile and efficient method is illustrated to obtain low volume resistivity (10^{-4} Ω·cm) with a small amount of AgNWs (<10 vol %) by serving AgNWs/LDH nanosheets hybrids as nanoscale conductive filler. Figure 4a demonstrates the influence of hybrid filler with different proportion of AgNWs to LDH nanosheets on the electrical property of composites. As can be seen, all samples incorporated with AgNWs/LDH nanosheets hybrids show lower resistivity than that of those filled with AgNWs only, and the resistivity reaches $(2.5 \pm 0.3) \times 10^{-4}$ Ω·cm when the proportion of AgNWs and LDH nanosheets is 4:1 while the blank sample is about 900 Ω·cm. Also, the resistivity is $(2.6 \pm 0.3) \times 10^{-3}$ Ω·cm when the proportion of AgNWs and LDH nanosheets is 1:1, demonstrating excess LDH nanosheets will decrease the contact between AgNWs. By using AgNWs/LDH nanosheets hybrids as nanoscale conductive filler, one can decrease the percolation threshold from 10.8 vol % (55 wt %) to 3.1 vol % (23.8 wt %) (Figure 4b) and reach very low resistivity (10^{-4} Ω·cm) only filled with 8.3 vol % AgNWs (see Supporting Information Table S1). As a contrast, 18.8 vol % AgNWs are needed to achieve 10^{-4} Ω·cm if pure AgNWs serve as fillers.

The fillers distribution in polymer matrix plays a crucial role in evaluating the properties of composites; thus, the structure of composites was analyzed to illuminate the mechanism of conductivity improvement. Similar to the pristine AgNWs deposited on glass slides (Supporting Information Figure S1), AgNWs aggregate to bundles without LDH nanosheets due to the strong depletion-induced interaction among AgNWs (see Figure 5a and b and the EDX spectrum (Figure 5c) of selected area). However, after hybridizing with LDH nanosheets and serving as conductive filler, the bundles of AgNWs disappear and the dispersion of AgNWs is improved due to the depletion-induced interaction among AgNWs being weakened and AgNWs

DOI: 10.1021/acsami.5b03824
ACS Appl. Mater. Interfaces 2015, 7, 14182−14191

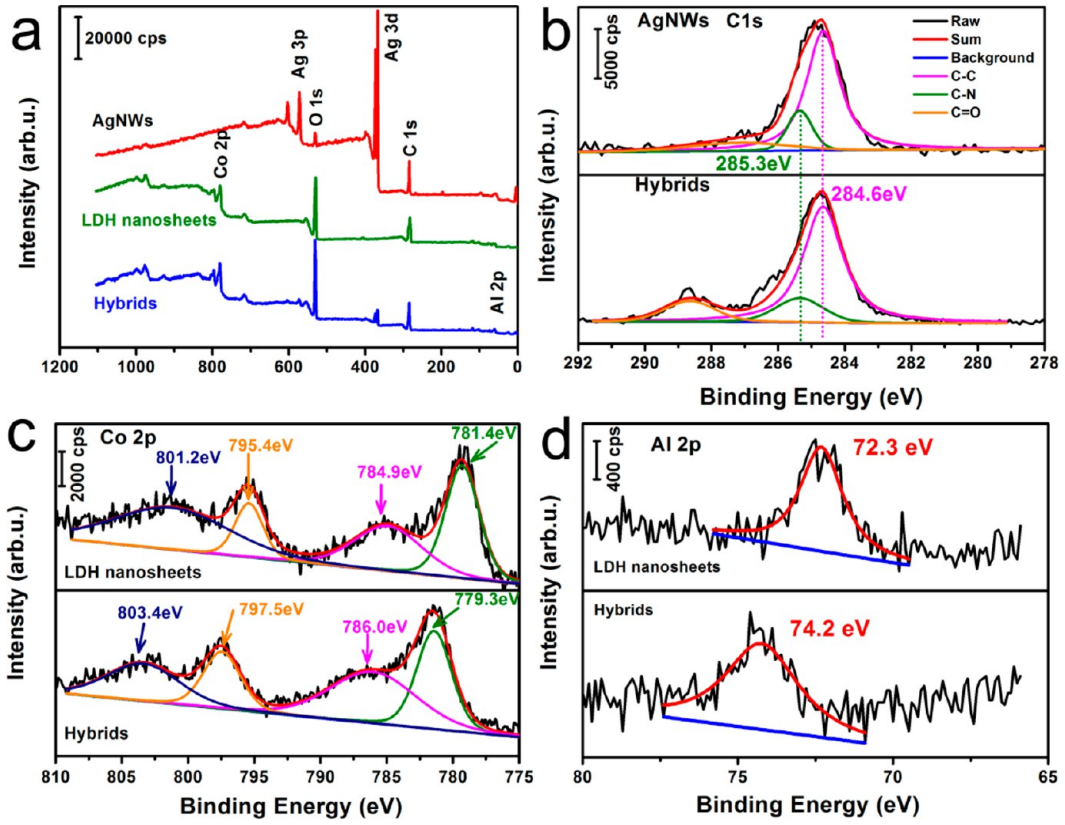

Figure 3. (a) XPS wide-scan spectra of AgNWs, LDH nanosheets, and AgNWs/LDH nanosheets hybrids; high-resolution XPS spectra of (b) C 1s for AgNWs and the hybrids, (c) Co 2p for LDH nanosheets and the hybrids, and (d) Al 2p for LDH nanosheets and the hybrids.

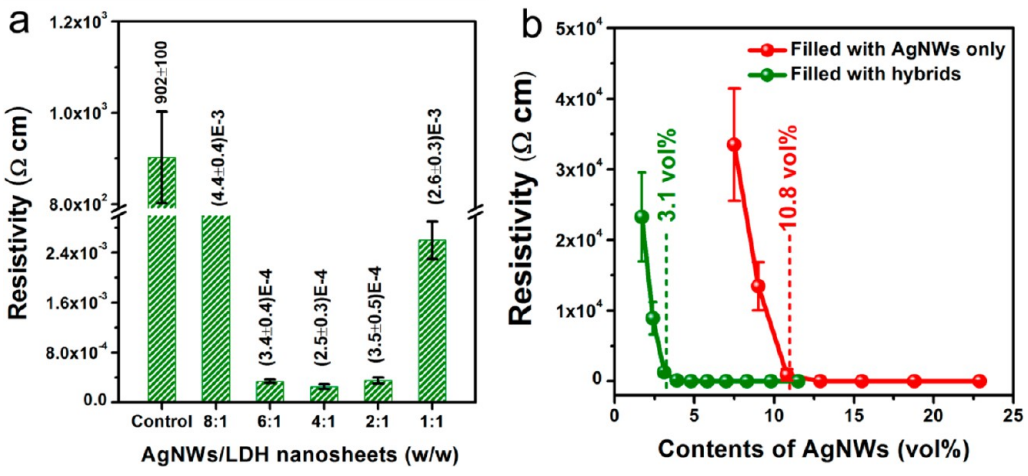

Figure 4. (a) Volume resistivity of composites filled with hybrids with different proportion of AgNWs to LDH nanosheets (the mass ratio of WPU and AgNWs was kept at 1:1 in all samples). (b) Volume resistivity of the composites as a function of contents of AgNWs (for the composites incorporated with the hybrids, the mass ratio of AgNWs and LDH nanosheets was kept at 4:1).

being divided by LDH nanosheets, resulting in a random AgNWs conductive network (see Figure 5d and e). Figure 5f shows the corresponding EDX spectrum of selected area in Figure 5e, showing that the white lines in Figure 5e are the LDH nanosheets. The hybrid network constructed by AgNWs and LDH nanosheets improves the dispersion of AgNWs in polymer matrix and makes it more likely to form an effective percolating network under a small amount of AgNWs which still obtain lower volume resistivity ($<10^{-4}$ Ω·cm), which is required for circuits in industry.

Plastic substrate has been always considered as an ideal substrate, but recent studies reveal that paper substrate offers new opportunities to fabricate the next generation of flexible devices due to its recyclability, mechanical flexibility, and light weight.[34] In this study, a rollerball pen (ball diameter is 0.7 mm) loaded with the as-prepared conductive ink can write on a common office paper, and conductive text or tracks with width about 500 μm were obtained (Figure 6a–f). Figure 6g shows the apparent viscosity (η, tested at 25 °C and 1 atm and the shear rate of 1 s^{-1}) of the ink as a function of the concentration of AgNWs/LDH nanosheets hybrids. The apparent viscosity of waterborne

DOI: 10.1021/acsami.5b03824
ACS Appl. Mater. Interfaces 2015, 7, 14182–14191

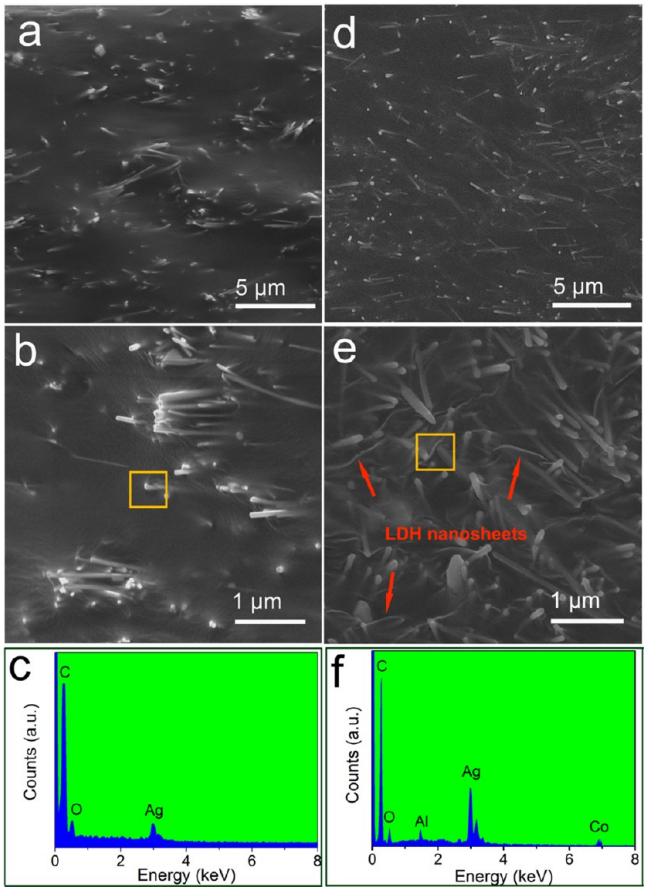

Figure 5. FESEM images of composites filled with AgNWs (a, b) and AgNWs/LDH nanosheets hybrids (d, e) with different magnifications; (c) and (f) are the EDAX spectra of the selected area corresponding to (b) and (e).

polyurethane (30 wt %) is about 0.07 Pa·s, and that of the ink-incorporated 10 wt % hybrids is around 0.8 Pa·s. To avoid leaking, skipping, or clogging while writing, a viscosity of 1−10 Pa·s is required.[35] In this study, the apparent viscosity of those inks with 20−60 wt % hybrids was between 1.5 and 4.5 Pa·s, which make it possible to manufacture the ink on paper substrate via writing and other methods such as inkjet printing and screen printing. To investigate the foldability of the conductive lines, a simple electric circuit was written on office paper and supported with an LED (Figure 6h, the operating voltage was 6 V); Figure 6i shows that the LED still works and the brightness does not change after the electric circuit is folded and weighted with 500 g on the top.

Performance of the Bending Sensor. The bending sensor fabricated on office paper by screen printing demonstrates extreme bending stability. The bendability was measured by bending the sensor with a radius of 0.5 cm and frequency of 4 Hz. The real-time resistance as a function of time was recorded and presented in Figure 7a, which shows that the electrical resistance of the sensor remains unchanged after over 3000 bending cycles. In contrast, the electrical resistance of the sensor using silver flakes as filler dramatically increases after only 10 bending cycles (Supporting Information Figure S8a). In addition, a minimal electrical resistance is observed for composites filled with hybrids while a maximum is recorded for composites filled with silver flakes in each bending cycle (inset in Figure 7a and Supporting Information Figure S8a). The mechanism of this phenomenon can be explained by tunneling resistance (R_{tunnel}) between fillers according the following formula[4,36]

$$R_{tunnel} = \frac{V}{AJ} = \frac{h^2 d}{Ae^2\sqrt{2m\lambda}}\exp\left(\frac{4\pi d}{h}\sqrt{2m\lambda}\right)$$

where V is the electrical potential difference, J is the tunneling current density, and A is the cross-sectional area of the tunnel; d is the distance of fillers; h is Planck's constant; λ is the height of the energy barrier; e is the quantum of electricity; and m is the mass of electron. The AgNWs conductive network is condensed under bending deformation that reduces the distance between AgNWs (Figure 7b). However, the conductive network connected by spherical or flaky microsized conductive fillers is negatively affected due to the distance between conductive fillers increasing under bending state (Supporting Information Figure S8b), which gives rise to increasing the tunneling resistance and limiting the tunneling current.

The above discussions reveal that the composites incorporated with the hybrids manufactured on paper have a good bending stability that can be used as bending sensor. Therefore, the capability of the sensor (composites filled with the hybrids) was studied, and the sensor response to the bending angle (θ) from 0° to 180° is illustrated in Figure 7c, which shows a high sensitivity (S) of 0.16 rad^{-1} ($S = \Delta R/R_0/\theta$) and a good liner fitting ($r = 0.9680$). Sensitivity and conductivity are the two most important parameters of piezoresistive materials, and it is challenging to satisfy both of them at the same time. The sensitivity of the sensor in this study is of the same order of magnitude as the sandwich-structured bending deformation sensor,[4] but our sensor also exhibits excellent conductivity. The resistivity of our bending sensor is as low as $(2.5 \pm 0.3) \times 10^{-4}$ Ω·cm, which is much lower than that of the previously reported AgNWs, graphene, CNTs, or ZnO-based piezoresistive sensors[2,4,8,37−41] and may be a potential candidate for low-voltage-driven wearable sensor systems.[42] However, the sensor prepared with composites without LDH nanosheets (18.8 vol % AgNWs was incorporated to make the resistivity reach 10^{-4} Ω·cm) shows very low sensitivity to bending deformation ($S = 0.03$ rad^{-1}). This is attributed to the higher volume fraction of AgNWs incorporated that forms a stable conductive network which is difficult to reconstruct at bending state. On the contrary, a relatively instable percolating network is formed with the introduction of LDH nanosheets, and the sparser AgNWs network is easier to be destructed and reconstructed in WPU matrix.[43] Additionally, the same electrical behavior and unchanged sensitivity of the sensor are observed even after 1000 "bending/relaxation" cycles (Figure 7d and e) due to the good flexibility of WPU which makes the AgNWs network fast to return to its original state after the strain is removed. The response and relaxation time of the sensor tested in this research are about 120 and 105 ms, respectively (Figure 7f).

Owing to the extreme bending stability and good sensitivity, the bending sensor can be used for a wearable and flexible sensing system mounted onto human bodies to monitor the motions or movements. Even through human motion detection sensors with similar materials have been developed in recent years, the bending sensor reported in this research is also highly conductive, low-cost, and environmentally friendly, which make large-scale and large-area preparation possible. To demonstrate the feasibility of the composites as a wearable bending sensor, the real-time detection is present in Figure 8. As indicated in Figure 8, the index finger of the person under test

DOI: 10.1021/acsami.5b03824
ACS Appl. Mater. Interfaces 2015, 7, 14182−14191

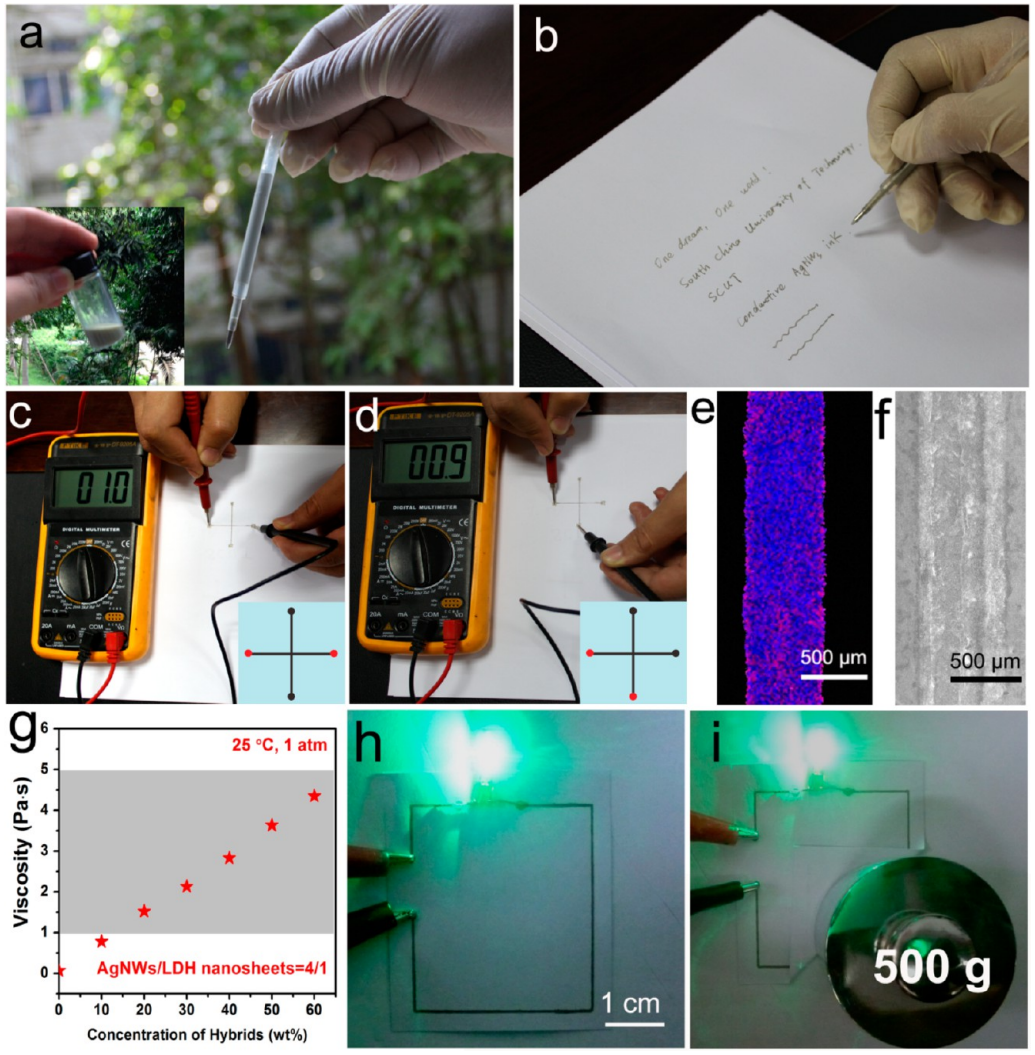

Figure 6. (a) Digital photograph of rollerball pen (ball diameter is 0.7 mm) loaded with conductive ink; inset is the typical digital photograph of conductive ink. (b) Conductive text written on an office paper by the rollerball pen. (c, d) Digital photographs of written tracks on office paper and resistance measurement. (e, f) Optical and SEM images of the written conductive line, respectively. (g) Apparent viscosity (η) of nanocomposites as a function of the concentration of hybrids (η was measured under 25 °C and 1 atm). (h) Simple paper-based electric circuit written by the rollerball pen; it still work after being folded and weighted with 500 g on the top (i).

was kept straight naturally; the bending sensor was under a moderate tension strain when the index finger had a moderate curvature, leading to a decrease in resistance. After the index finger straightened, the sensor relaxed and the strain decreased, accompanied by an increase in resistance and a return to original state. By mounting the sensor on the other four fingers, the sensor can also monitor the motions or movements as well (Figure 8c). As one of the most frequently used joints, it is of importance to detect or simulate the motion of the elbow joint. In this research, the bending sensor was attached onto the inner margin of the elbow joint while the volunteer straightened the arm naturally. Initially the sensor was in relaxation state, and a maximum resistance was observed (Figure 8d). After the arm was bent to about 90°, the resistance suddenly decreased (about 20%) due to tension generated during the bending process, and a larger decrease in resistance was observed (about 40%) when the arm continued to bend to 160°. When the arm was straightened, the resistance returned to the initial value. All the results reveal that the bending sensor in this study exhibits good repeatability, stability, and responsiveness and could meet the needs in numerous applications for robotic systems.

CONCLUSION

In this study, hybrids of AgNWs and LDH nanosheets were prepared, and results reveal that nonconductive LDH nanosheets are embedded into AgNWs network and LDH nanosheets assist the dispersion of AgNWs in polymer matrix. With introduction of LDH nanosheets, the percolation threshold of the composites decreases from 10.8 vol % (55 wt %) to 3.1 vol % (23.8 wt %) and the resistivity reaches 10^{-4} Ω·cm only incorporated with 8.3 vol % AgNWs due to the dispersion improvement of AgNWs. The as-prepared composites with low percolation threshold could be manufactured on paper by various methods such as rollerball pen writing, screen printing, and inkjet printing. In addition, a simple but efficient paper-based bending sensor with low cost, good conductivity (10^{-4} Ω·cm) and sensitivity (0.16 rad^{-1}), fast response (120 ms) and relaxation time (105 ms), extreme bending stability (>3000 cycles), and nontoxicity has been developed to monitor the human motions and shows good repeatability and stability.

DOI: 10.1021/acsami.5b03824
ACS Appl. Mater. Interfaces 2015, 7, 14182−14191

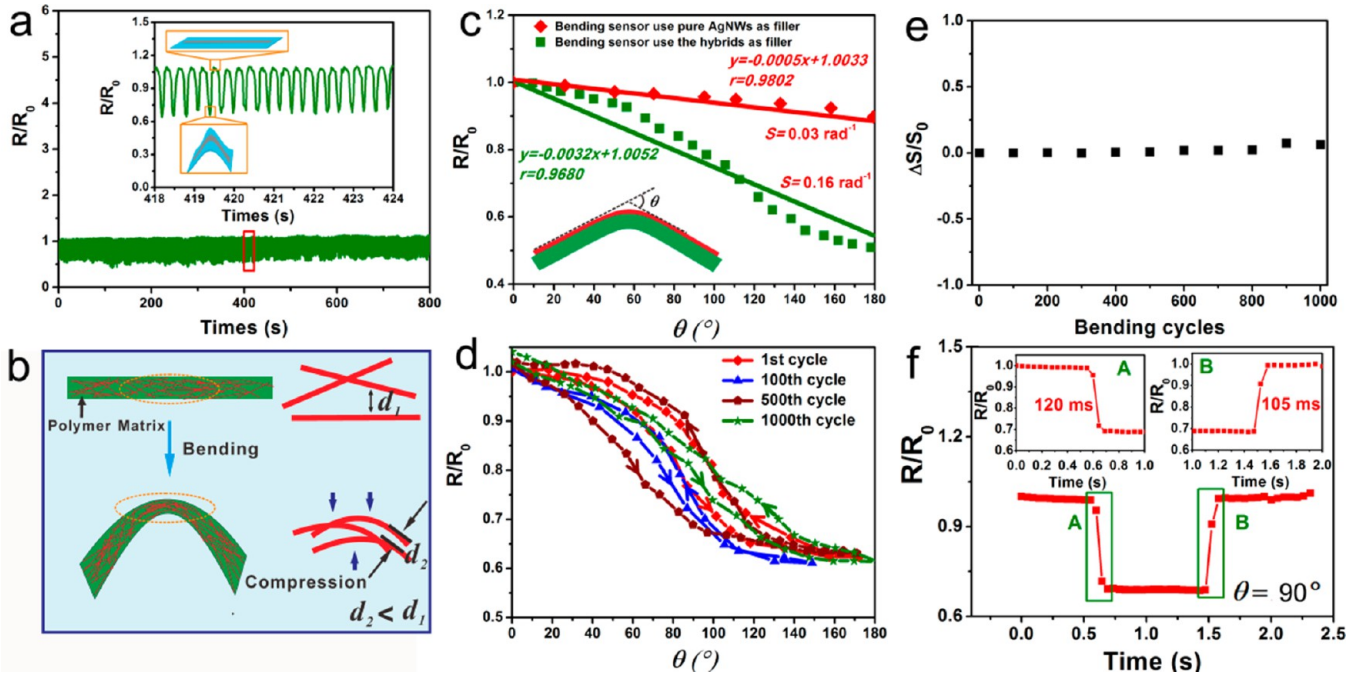

Figure 7. (a) Responses of the paper-based bending sensor to the bending cycles under the frequency of 4 Hz. (b) Schematic to show the effect of bending on the AgNWs network. (c) Response of the sensor to the bending angle from 0° to 180° and (d) the repeated bending/relaxation cycles. Normalized sensitivity of sensor as a function of bending cycles (e). (f) Fast response (120 ms) and relaxation time (105 ms) of the sensor.

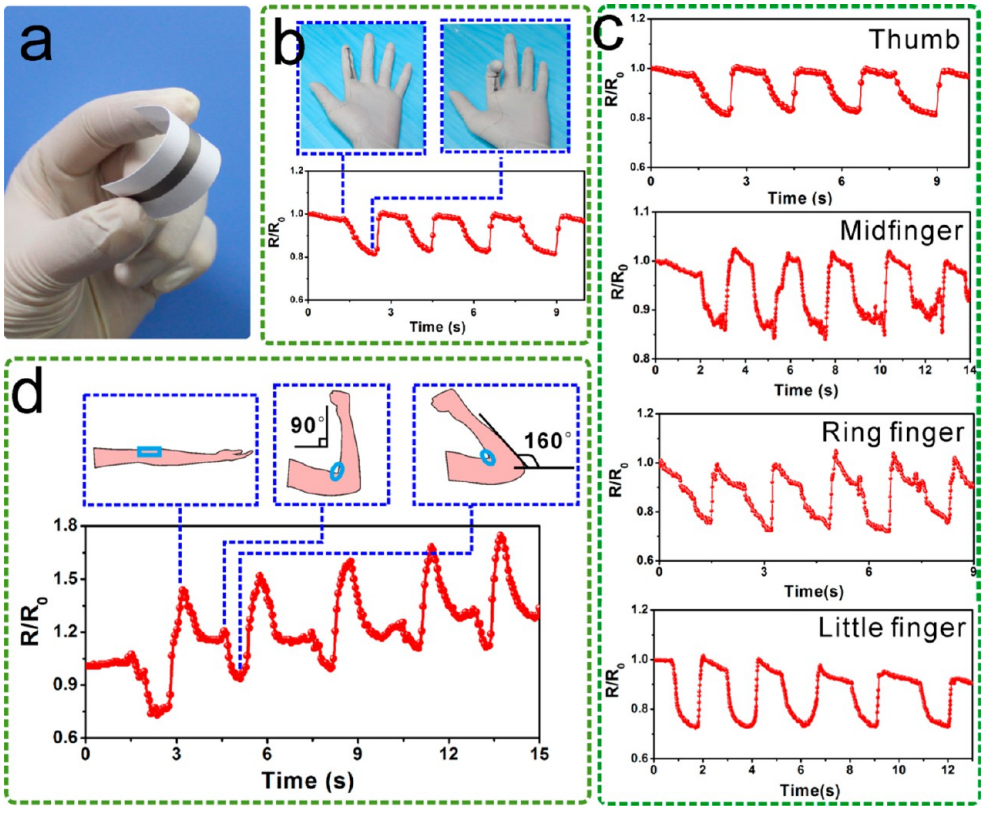

Figure 8. Digital photograph of the bending sensor (a). Demonstrations and results of motion detection of the index finger (b) and the other four fingers (c). Motion detection of the elbow joint (d).

■ ASSOCIATED CONTENT

Supporting Information

Synthesis and anion exchange of Co−Al LDHs; FESEM images of pristine AgNWs and histogram showing length and diameter of AgNWs; XRD results of pristine AgNWs; schematic illustration of anion exchange of Co−Al LDHs; FTIR patterns, XRD results, and FESEM images of Co−Al LDHs intercalated with different anions; the digital photograph and Tyndall effect of

DOI: 10.1021/acsami.5b03824
ACS Appl. Mater. Interfaces 2015, 7, 14182−14191

the LDH nanosheets suspensions; UV−vis spectra of AgNWs, LDH nanosheets, and AgNWs/LDH nanosheets hybrids; responses of the composites incorporated with silver flakes; volume resistivity of the composites filled with the hybrids and AgNWs only. The Supporting Information is available free of charge on the ACS Publications website at DOI: 10.1021/acsami.5b03824.

AUTHOR INFORMATION

Corresponding Author

*E-mail: psliulan@scut.edu.cn.

Notes

The authors declare no competing financial interest.

ACKNOWLEDGMENTS

This work was financially supported by National Basic Research Program of China, Grant No. 2015CB654700 (2015CB674703), National Natural Science Foundation of China Based United Fund Guangdong Province (U1134005), Science and Technology Innovation Key Project of Universities of Guangdong province (CXZD1106), and Strategic New Industry Core Technology Research Project of Guangdong Province (2012A090100017).

REFERENCES

(1) Cattin, C.; Hubert, P. Piezoresistance in Polymer Nanocomposites with High Aspect Ratio Particles. *ACS Appl. Mater. Interfaces* **2014**, *6*, 1804−1811.

(2) Yan, C.; Wang, J.; Kang, W.; Cui, M.; Wang, X.; Foo, C. Y.; Chee, K. J.; Lee, P. S. Highly Stretchable Piezoresistive Graphene−Nanocellulose Nanopaper for Strain Sensors. *Adv. Mater.* **2014**, *26*, 2022−2027.

(3) Yao, H. B.; Ge, J.; Wang, C. F.; Wang, X.; Hu, W.; Zheng, Z. J.; Ni, Y.; Yu, S. H. A Flexible and Highly Pressure-Sensitive Graphene−Polyurethane Sponge Based on Fractured Microstructure Design. *Adv. Mater.* **2013**, *25*, 6692−6698.

(4) Amjadi, M.; Pichitpajongkit, A.; Lee, S.; Ryu, S.; Park, I. Highly Stretchable and Sensitive Strain Sensor Based on Silver Nanowire−Elastomer Nanocomposite. *ACS Nano* **2014**, *8*, 5154−5163.

(5) Zhao, S.; Gao, Y.; Li, J.; Zhang, G.; Zhi, C.; Deng, L.; Sun, R.; Wong, C. P. Layer-by-Layer Assembly of Multifunctional Porous N-Doped Carbon Nanotube Hybrid Architectures for Flexible Conductors and Beyond. *ACS Appl. Mater. Interfaces* **2015**, *7*, 6716−6723.

(6) Wang, J.; Jiu, J.; Nogi, M.; Sugahara, T.; Nagao, S.; Koga, H.; He, P.; Suganuma, K. A Highly Sensitive and Flexible Pressure Sensor with Electrodes and Elastomeric Interlayer Containing Silver Nanowires. *Nanoscale* **2015**, *7*, 2926−2932.

(7) Lee, S.; Shin, S.; Lee, S.; Seo, J.; Lee, J.; Son, S.; Cho, H. J.; Algadi, H.; Al-Sayari, S.; Kim, D. E.; Lee, T. Ag Nanowire Reinforced Highly Stretchable Conductive Fibers for Wearable Electronics. *Adv. Funct. Mater.* **2015**, *25*, 3114−3121.

(8) Ha, M.; Lim, S.; Park, J.; Um, D. S.; Lee, Y.; Ko, H. Bioinspired Interlocked and Hierarchical Design of ZnO Nanowire Arrays for Static and Dynamic Pressure-Sensitive Electronic Skins. *Adv. Funct. Mater.* **2015**, *25*, 2841−2849.

(9) Huang, G. W.; Xiao, H. M.; Fu, S. Y. Paper-Based Silver-Nanowire Electronic Circuits with Outstanding Electrical Conductivity and Extreme Bending Stability. *Nanoscale* **2014**, *6*, 8495−8502.

(10) Nogi, M.; Komoda, N.; Otsuka, K.; Suganuma, K. Foldable Nanopaper Antennas for Origami Electronics. *Nanoscale* **2013**, *5*, 4395−4399.

(11) Siegel, A. C.; Phillips, S. T.; Wiley, B. J.; Whitesides, G. M. Thin, Lightweight, Foldable Thermochromic Displays on Paper. *Lab Chip* **2009**, *9*, 2775−2781.

(12) Chun, K. Y.; Oh, Y.; Rho, J.; Ahn, J. H.; Kim, Y. J.; Choi, H. R.; Baik, S. Highly Conductive, Printable, and Stretchable Composite Films of Carbon Nanotubes and Silver. *Nat. Nanotechnol.* **2010**, *5*, 853−857.

(13) Xu, F.; Zhu, Y. Highly Conductive and Stretchable Silver Nanowire Conductors. *Adv. Mater.* **2012**, *24*, 5117−5122.

(14) Song, L.; Myers, A. C.; Adams, J. J.; Zhu, Y. Stretchable and Reversibly Deformable Radio Frequency Antennas Based on Silver Nanowires. *ACS Appl. Mater. Interfaces* **2014**, *6*, 4248−4253.

(15) Li, Z.; Zhang, R.; Moon, K. S.; Liu, Y.; Hansen, K.; Le, T.; Wong, C. P. Highly Conductive, Flexible, Polyurethane-Based Adhesives or Flexible and Printed Electronics. *Adv. Funct. Mater.* **2013**, *23*, 1459−1465.

(16) Kwon, S.; Ma, R.; Kim, U.; Choi, H. R.; Baik, S. Flexible Electromagnetic Interference Shields Made of Silver Flakes, Carbon Nanotubes, and Nitrile Butadiene Rubber. *Carbon* **2014**, *68*, 118−124.

(17) Park, M.; Park, J.; Jeong, U. Design of Conductive Composite Elastomers for Stretchable Electronics. *Nano Today* **2014**, *9*, 244−260.

(18) Zhao, H.; Bai, J. Highly Sensitive Piezo-Resistive Graphite Nanoplatelet−Carbon Nanotubes Hybrids/Polydimethylsilicone Composites with Improved Conductive Network Construction. *ACS Appl. Mater. Interfaces* **2015**, *7*, 9652−9659.

(19) Duan, L.; Fu, S.; Deng, H.; Zhang, Q.; Wang, K.; Chen, F.; Fu, Q. The Resistivity−Strain Behavior of Conductive Polymer Composites: Stability and Sensitivity. *J. Mater. Chem. A* **2014**, *2*, 17085−17098.

(20) Gelves, G. A.; Lin, B.; Sundararaj, U.; Haber, J. A. Low Electrical Percolation Threshold of Silver and Copper Nanowires in Polystyrene Composites. *Adv. Funct. Mater.* **2006**, *16*, 2423−2430.

(21) Nam, S.; Cho, H. W.; Lim, S.; Kim, D.; Kim, H.; Sung, B. J. Enhancement of Electrical and Thermomechanical Properties of Silver Nanowire Composites by the Introduction of Nonconductive Nanoparticles: Experiment and Simulation. *ACS Nano* **2013**, *7*, 851−856.

(22) Luan, V. H.; Tien, H. N.; Cuong, T. V.; Kong, B. S.; Chung, J. S.; Kim, E. J.; Hur, S. H. Novel Conductive Epoxy Composites Composed of 2-D Chemically Reduced Graphene and 1-D Silver Nanowire Hybrid Fillers. *J. Mater. Chem.* **2012**, *22*, 8649−8653.

(23) Yang, C.; Gu, H.; Lin, W.; Yuen, M. M.; Wong, C. P.; Xiong, M.; Gao, B. Silver Nanowires: From Scalable Synthesis to Recyclable Foldable Electronics. *Adv. Mater.* **2011**, *23*, 3052−3056.

(24) Hibino, T.; Ohya, H. Synthesis of Crystalline Layered Double Hydroxides: Precipitation by Using Urea Hydrolysis and Subsequent Hydrothermal Reactions in Aqueous Solutions. *Appl. Clay Sci.* **2009**, *45*, 123−132.

(25) Liu, Z.; Ma, R.; Osada, M.; Iyi, N.; Ebina, Y.; Takada, K.; Sasaki, T. Synthesis, Anion Exchange, and Delamination of Co−Al Layered Double Hydroxide: Assembly of the Exfoliated Nanosheet/Polyanion Composite Films and Magneto-Optical Studies. *J. Am. Chem. Soc.* **2006**, *128*, 4872−4880.

(26) Kota, A. K.; Cipriano, B. H.; Duesterberg, M. K.; Gershon, A. L.; Powell, D.; Raghavan, S. R.; Bruck, H. A. Electrical and Rheological Percolation in Polystyrene/MWCNT Nanocomposites. *Macromolecules* **2007**, *40*, 7400−7406.

(27) Yao, S.; Zhu, Y. Wearable Multifunctional Sensors Using Printed Stretchable Conductors Made of Silver Nanowires. *Nanoscale* **2014**, *6*, 2345−2352.

(28) Li, J.; Tang, S.; Lu, L.; Zeng, H. C. Preparation of Nanocomposites of Metals, Metal Oxides, and Carbon Nanotubes via Self-Assembly. *J. Am. Chem. Soc.* **2007**, *129*, 9401−9409.

(29) Fan, G.; Wang, H.; Xiang, X.; Li, F. Co−Al Mixed Metal Oxides/Carbon Nanotubes Nanocomposite Prepared via a Precursor Route and Enhanced Catalytic Property. *J. Solid State Chem.* **2013**, *197*, 14−22.

(30) Sun, Y.; Yin, Y.; Mayers, B. T.; Herricks, T.; Xia, Y. Uniform Silver Nanowires Synthesis by Reducing $AgNO_3$ with Ethylene Glycol in the Presence of Seeds and Poly(vinyl pyrrolidone). *Chem. Mater.* **2002**, *14*, 4736−4745.

(31) Xia, Y.; Xiong, Y.; Lim, B.; Skrabalak, S. E. Shape-Controlled Synthesis of Metal Nanocrystals: Simple Chemistry Meets Complex Physics? *Angew. Chem., Int. Ed.* **2009**, *48*, 60−103.

(32) Wei, Y.; Chen, S.; Li, F.; Liu, K.; Liu, L. Hybrids of Silver Nanowires and Silica Nanoparticles as Morphology Controlled Conductive Filler Applied in Flexible Conductive Nanocomposites. *Composites, Part A* **2015**, *73*, 195−203.

DOI: 10.1021/acsami.5b03824
ACS Appl. Mater. Interfaces 2015, 7, 14182−14191

(33) Nicolosi, V.; Chhowalla, M.; Kanatzidis, M. G.; Strano, M. S.; Coleman, J. N. Liquid Exfoliation of Layered Materials. *Science* **2012**, *340*, 1226419.
(34) Preston, C.; Fang, Z.; Murray, Jo.; Zhu, H.; Dai, J.; Munday, J. N.; Hu, L. B. Silver Nanowire Transparent Conducting Paper-Based Electrode with High Optical Haze. *J. Mater. Chem. C* **2014**, *2*, 1248−1254.
(35) Russo, A.; Ahn, B. Y.; Adams, J. J.; Duoss, E. B.; Bernhard, J. T.; Lewis, J. A. Pen-on-Paper Flexible Electronics. *Adv. Mater.* **2011**, *23*, 3426−3430.
(36) Hu, N.; Karube, Y.; Yan, C.; Masuda, Z.; Fukunaga, H. Tunneling Effect in a Polymer/Carbon Nanotube Nanocomposite Strain Sensor. *Acta Mater.* **2008**, *56*, 2929−2936.
(37) Boland, C. S.; Khan, U.; Backes, C.; O'Neill, A.; McCauley, J.; Duane, S.; Shanker, R.; Liu, Y.; Jurewicz, I.; Dalton, A. B.; Coleman, J. N. Sensitive, High-Strain, High-Rate Bodily Motion Sensors Based on Graphene Rubber Composites. *ACS Nano* **2014**, *8*, 8819−8830.
(38) Yang, P.; Lin, L.; Yi, F.; Li, X.; Pradel, K. C.; Zi, Y.; Wu, C. I.; He, J. H.; Zhang, Y.; Wang, Z. L. A Flexible, Stretchable, and Shape-Adaptive Approach for Versatile Energy Conversion and Self-Powered Biomedical Monitoring. *Adv. Mater.* **2015**, DOI: 10.1002/adma.201500652.
(39) Park, J.; Lee, Y.; Hong, J.; Ha, M.; Jung, Y. D.; Lim, H.; Kim, S. Y.; Ko, H. Giant Tunneling Piezoresistance of Composite Elastomers with Interlocked Microdome Arrays for Ultrasensitive and Multimodal Electronic Skins. *ACS Nano* **2014**, *8*, 4689−4697.
(40) Park, J.; Lee, Y.; Hong, J.; Lee, Y.; Ha, M.; Jung, Y.; Lim, H.; Kim, S. Y.; Ko, H. Tactile-Direction-Sensitive and Stretchable Electronic Skins Based on Human-Skin-Inspired Interlocked Microstructures. *ACS Nano* **2014**, *8*, 12020−12029.
(41) Wang, X. W.; Gu, Y.; Xiong, Z.; Cui, Z.; Zhang, T. Silk-Molded Flexible, Ultrasensitive, and Highly Stable Electronic Skin for Monitoring Human Physiological Signals. *Adv. Mater.* **2014**, *26*, 1336−1342.
(42) Sun, Q.; Seung, W.; Kim, B. J.; Seo, S.; Kim, S. W.; Cho, J. H. Active Matrix Electronic Skin Strain Sensor Based on Piezopotential-Powered Graphene Transistors. *Adv. Mater.* **2015**, *27*, 3411−3417.
(43) Hou, Y.; Wang, D.; Zhang, X. M.; Zhao, H.; Zha, J. W.; Dang, Z. M. Positive Piezoresistive Behavior of Electrically Conductive Alkyl-Functionalized Graphene/Polydimethylsilicone Nanocomposites. *J. Mater. Chem. C* **2013**, *1*, 515−521.

DOI: 10.1021/acsami.5b03824
ACS Appl. Mater. Interfaces 2015, 7, 14182−14191